Polycomb Repressive Complex 1 Controls Maintenance of Fungiform Papillae by Repressing Sonic Hedgehog Expression

Carmit Bar[1], **Idan Cohen**[1], **Dejian Zhao**[2,8,9], **Venu Pothula**[1], **Anna Litskevitch**[3], **Haruhiko Koseki**[4,5], **Deyou Zheng**[2,6,7], **Elena Ezhkova**[1,10,*]

[1]Black Family Stem Cell Institute, The Tisch Cancer Institute, Department of Cell, Developmental, and Regenerative Biology, Icahn School of Medicine at Mount Sinai, 1 Gustave L. Levy Place, New York, NY 10029, USA

[2]Department of Genetics, Albert Einstein College of Medicine, 1300 Morris Park Avenue, Bronx, NY 10461, USA

[3]Department of Molecular & Cell Biology, University of California, Berkeley, 142 Life Sciences Addition, Berkeley, CA 94720, USA

[4]Laboratory for Developmental Genetics, RIKEN Center for Integrative Medical Sciences (RIKEN-IMS), 1-7-22 Suehiro-cho, Tsurumi-ku, Yokohama 230-0045, Japan

[5]AMED-CREST, 1-7-22 Suehiro-cho, Tsurumi-ku, Yokohama 230-0045, Japan

[6]Department of Neurology, Albert Einstein College of Medicine, 1300 Morris Park Avenue, Bronx, NY 10461, USA

[7]Department of Neuroscience, Albert Einstein College of Medicine, 1300 Morris Park Avenue, Bronx, NY 10461, USA

[8]Present address: Department of Genetics, Yale University School of Medicine, 333 Cedar St., New Haven, CT 06510, USA

[9]Present address: Yale Center for Genome Analysis, Yale University, New Haven, CT 06510, USA

[10]Lead Contact

SUMMARY

How tissue patterns are formed and maintained are fundamental questions. The murine tongue epithelium, a paradigm for tissue patterning, consists of an array of specialized fungiform papillae structures that harbor taste cells. The formation of fungiform papillae is preceded by pronounced

spatial changes in gene expression, in which taste cell genes such as *Shh*, initially diffused in lingual epithelial progenitors, become restricted to taste cells when their specification progresses. However, the requirement of spatial restriction of taste cell gene expression for patterning and formation of fungiform papillae is unknown. Here, we show that a chromatin regulator, Polycomb repressive complex (PRC) 1, is required for proper maintenance of fungiform papillae by repressing *Shh* and preventing ectopic SHH signaling in non-taste cells. Ablation of SHH signaling in PRC1-null non-taste cells rescues the maintenance of taste cells. Altogether, our studies exemplify how epigenetic regulation establishes spatial gene expression patterns necessary for specialized niche structures.

Graphical Abstract
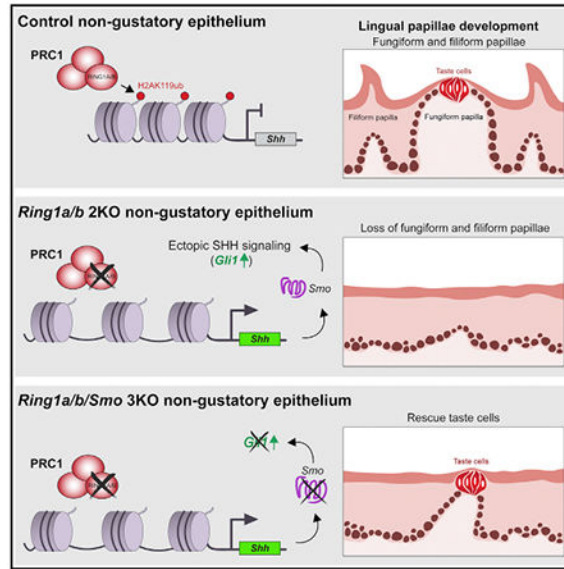
In Brief

Formation and maintenance of patterns are critical for tissue development. Bar et al. show that PRC1, an epigenetic regulator, is critical for lingual papillae development. Specifically, PRC1 regulates maintenance of the developing fungiform papillae, harboring taste cells, by repressing *Shh* expression in the non-gustatory epithelium surrounding taste cells.

INTRODUCTION

Tissue patterning is a fundamental process in animal development in which initially identical cells become organized into distinct domains. For example, lingual papillae, teeth, mammary glands, and hair follicles are highly patterned structures, all originating from a single layer of embryonic epithelial progenitors. These structures provide essential functions for survival and confer structural complexity to the otherwise flat epithelium (Biggs and Mikkola, 2014; Misra et al., 2017). However, little is known about the processes controlling their patterning and maintenance.

The unique structure of the murine lingual epithelium makes it a great model system to study tissue patterning. It is organized as a patterned array of lingual papillae called fungiform and filiform papillae (Mbiene and Roberts, 2003; Okubo et al., 2006). The fungiform papillae harbor the taste cells (Barlow and Klein, 2015; Kapsimali and Barlow, 2013; Mistretta and Kumari, 2017) and are surrounded by non-gustatory filiform papillae that provide protective barrier functions and help in food intake (Manabe et al., 1999). During development, the lingual papillae originate from a single layer of lingual epithelial progenitors. From embryonic day (E) 10 to E11, before induction of lingual papillae, lingual epithelial progenitors appear identical and express low levels of the taste cell-specific genes *Wnt10b*, *Shh*, and *Sox2* (Hall et al., 1999; Iwatsuki et al., 2007; Liu et al., 2007; Okubo et al., 2006; Figure 1A). At E12.5, the expression of taste cell genes becomes restricted to taste placodes that will give rise to taste cells and is downregulated in the remaining areas of the non-gustatory epithelium (Iwatsuki et al., 2007; Okubo et al., 2006; Thirumangalathu et al., 2009).

Spatial changes in gene expression are necessary for proper development of the tongue and taste system. Before formation of taste placodes, diffused Sonic Hedgehog (SHH) expression is critical for tongue formation (Liu et al., 2004). When taste cells specify at E12.5, WNT10B in the taste placode activates canonical WNT signaling, inducing high *Shh* expression in taste cells (Iwatsuki et al., 2007). SHH, in turn, functions as a negative regulator of taste cell patterning, repressing taste cell fate, because inhibition of SHH signaling results in formation of ectopic and enlarged fungiform papillae (Hall et al., 2003; Mistretta et al., 2003).

How spatial changes in expression of taste lineage genes are established, how the repression of taste cell genes in the non-gustatory epithelium is controlled, and whether these processes are critical for lingual papillae patterning and development are unanswered questions.

Here, in a search for transcriptional repressors that play a role in lingual pattern formation, we studied the role of the Polycomb complexes in the developing tongue. The Polycomb complexes are key transcriptional repressors that act as two multi-subunit complexes, Polycomb repressive complex (PRC) 1 and 2 (Bracken and Helin, 2009). PRC2 consists of three core subunits, EZH1/2, EED, and SUZ12, and catalyzes tri-methylation of histone H3 lysine 27 (H3K27me3) (Cao et al., 2002; Margueron and Reinberg, 2011). PRC1 contains an E3 ubiquitin ligase, RING1A or RING1B, which is involved in histone H2A lysine 119 ubiquitination (H2AK119ub) (de Napoles et al., 2004; Gao et al., 2012; Wang et al., 2004). The catalytic activity of PRC1 has been shown to play a role in gene repression (Cohen et al., 2018; Endoh et al., 2012; Kallin et al., 2009; Wang et al., 2004). PRC1 and PRC2 together mediate chromatin compaction, resulting in gene silencing (Cao et al., 2002; Min et al., 2003; Simon et al., 1992; Simon and Kingston, 2009, 2013). Both PRC2 and PRC1 are critical in the regulation of cell identity during early development, as well as the identity of adult stem cells in multiple tissue types (Boyer et al., 2006; Chiacchiera et al., 2016; Cohen et al., 2018; Endoh et al., 2012, 2017a, 2017b; Ezhkova et al., 2009; Juan et al., 2011).

Here, we identified critical roles for PRC1 in lingual papillae morphogenesis and patterning. PRC2 function is dispensable. By performing genetic loss-of-function studies, coupled with

genome-wide transcriptional and chromatin analyses, we determined the role of PRC1-mediated gene repression in the establishment of the *Shh* expression pattern, which is critical for lingual papillae morphogenesis and patterning.

RESULTS

PRC1 Is Critical for Lingual Papillae Development, whereas PRC2 Is Dispensable

To test whether PRC1 regulates lingual epithelium morphogenesis and patterning (Figure 1A), we ablated the core PRC1 subunits, RING1A and RING1B, in the developing non-gustatory lingual epithelium. We achieved this by crossing *Ring1a* null *Ring1b-floxed* mice with *K14-Cre* mice, in which Cre recombinase is expressed under the keratin 14 promoter (*Ring1a/b* double knockout [2KO]). To visualize *K14-Cre* expression, we crossed *K14-Cre* mice with *Rosa26-mT/mG* reporter mice (Muzumdar et al., 2007). This reporter mouse globally expresses a membranal TOMATO fluorophore and a STOP codon flanked by *loxP* sequences, followed by a promoter-less membranal GFP fluorophore. Expression of *Cre* results in deletion of TOMATO and the STOP codon, as well as activation of GFP expression. Analysis of *K14-Cre::Rosa26-mT/mG* tongues showed that *K14-Cre* is active in the non-gustatory lingual epithelium cells, but not in taste cells (Figure 1B). *K14-Cre* recombination initially occurs at the tongue tip, while homogeneous targeting of the lingual epithelium is achieved by E14.5 (Ma et al., 2009). To determine when *Ring1b* is first ablated, we analyzed the expression of H2AK119ub and RING1B by immunofluorescence (IF) of *Ring1a/b* 2KO embryos and controls at E14.5 and E16. This analysis showed that starting only at E16, RING1B and H2AK119ub are lost in the non-gustatory epithelium cells, but not in the taste cells (Figures 1C, S1A, and S1B).

Fungiform papillae in *Ring1a/b* 2KO embryos appeared normal at E16. They were induced on the tongue surface, including the tip, with the taste cells localized to the top of the fungiform papilla structures, while the filiform papillae were not yet formed (Figures 1D, 1E, S1C, and S1D). We observed a slight upregulation of SOX2 in the non-gustatory epithelium in *Ring1a/b* 2KO embryos above the basal level (Figure 1E). At E17, as development progressed, fungiform papillae structures were partially disorganized in *Ring1a/b* null lingual epithelium when compared with control embryos, with flat clusters of K8(+) SOX2(+) taste cells (Figures 1F and 1G). By post-natal day 0 (P0), histological (H&E) and scanning electron microscopy (SEM) analyses revealed that the tongues of *Ring1a/b* 2KO mice lacked fungiform papillae and failed to form filiform papillae (Figures 1H and S1E). IF analysis confirmed the SEM and H&E data and showed that the number of cell clusters expressing K8 was drastically reduced in *Ring1a/b* 2KO lingual epithelium (Figures 1I and S1H). Thus, the fungiform papillae are not maintained, and the filiform papillae fail to form in *Ring1a/b* 2KO mice.

Gene expression analysis (RNA sequencing [RNA-seq]) in control E16 embryos shows that *Ring1a* and *Ring1b* are co-expressed in the lingual epithelium (Table S1). To confirm that *Ring1a* and *Ring1b* redundantly regulate the lingual epithelial morphogenesis and patterning, we analyzed *Ring1a* knockout (KO) and *Ring1b* conditional knockout (cKO) newborn mice. The H2AK119ub mark was present in the lingual epithelium of both *Ring1a* KO and *Ring1b* cKO mice (Figure S1I), and fungiform and filiform papillae were formed

similarly to those in controls (Figure S1J). These data show that *Ring1a* and *Ring1b* function redundantly in the lingual epithelium, and ablation of both genes is necessary for the loss of lingual papillae.

The core PRC2 subunits EED, SUZ12, and EZH1/2 are essential for PRC2 stability and function (Cao and Zhang, 2004; Dauber et al., 2016; Faust et al., 1995; Ketel et al., 2005; Pasini et al., 2004). Ablation of *Eed* in the lingual epithelium was sufficient to abolish the H3K27me3 mark (Figure S1K), but not the PRC1 mark (Figure S1L). Although PRC1 and PRC2 are thought to act together (Cao et al., 2002; Min et al., 2003; Simon et al., 1992; Simon and Kingston, 2009), normal fungiform and filiform papillae were observed in *Eed* cKO mice (Figures S1F–S1H). To test whether PRC2 and PRC1 cooperate in the development of lingual papillae, we generated *Ring1a/b/Eed* triple knockout (3KO) mice by crossing *Eed* cKO and *Ring1a/b* 2KO mice and found that the lingual epithelium of newborn *Ring1a/b/Eed* 3KO mice lacked both fungiform and filiform papillae, similar to *Ring1a/b* 2KO mice, and the additional loss of *Eed* did not exacerbate the *Ring1a/b* 2KO tongue phenotype (Figures S1F–S1H). Therefore, PRC1, but not PRC2, is critical for lingual papillae development.

Cell-Cycle Repressors and SHH Signaling Components Are Upregulated in PRC1 Null Non-gustatory Epithelium

To gain insight into the molecular mechanisms behind the Ring1a/b 2KO phenotype, we carried out RNA-seq analysis on fluorescence-activated cell sorting (FACS)-purified lingual epithelium from Ring1a/b 2KO and control E16 tongues (Figure S2). Differential gene expression analysis showed that 1,163 genes were upregulated in Ring1a/b 2KO compared with control lingual epithelial cells (Figure 2A; Table S1). Gene Ontology (GO) analysis (Huang da et al., 2009) of the upregulated genes showed enrichment for genes related to embryonic appendage morphogenesis, negative regulation of cellular proliferation, and the Smoothened (Smo) signaling pathway (Figure 2B; Table S2). We confirmed the upregulation of selected genes in the enriched categories by qRT-PCR (Figure 2C). Chromatin immunoprecipitation sequencing (ChIP-seq) for PRC1-dependent H2AK119ub in control lingual epithelium cells revealed that roughly 65% of the upregulated genes were direct targets of H2AK119ub (Figure 2D; Table S3). Altogether, these data indicate that PRC1 is required for gene repression in the developing lingual epithelium.

GO analysis of the 500 downregulated genes showed enrichment for epithelial cell development, epithelial cell differentiation, and tissue development pathways and pointed to a decrease in mitotic division (Figure 2E; Tables S1 and S2). We confirmed the downregulation of selected genes in the enriched categories by qRT-PCR (Figure 2F) and by IF staining (Figure 2G). Lingual epithelial-specific keratins *Krt6a, Krt6b* (Lessard and Coulombe, 2012; Rothnagel et al., 1999), and *Krt13* (Iwasaki et al., 2006) and lingual-specific transcription factor *Pax9,* which is essential for filiform papillae development (Jonker et al., 2004), were among the downregulated genes (Figures 2F and 2G; Table S1). These findings indicate a decrease in lingual keratinocyte identity, hinting at possible mechanisms leading to the loss of filiform papillae in *Ring1a/b* 2KO tongues.

Loss of Fungiform and Filiform Papillae in *Ring1a/b* 2KO Mice Is Not Caused by *Cdkn2a* Upregulation Alone

Consistent with the observed upregulation of negative regulators of cell cycle and downregulation of mitotic division genes in *Ring1a/b* 2KO lingual epithelium (Figures 2B, 2C, and 2E; Table S2), analysis of bromodeoxyuridine (BrdU) incorporation showed that proliferation was reduced in *Ring1a/b* 2KO lingual epithelium (Figures 3A and 3B). No changes in apoptosis were observed by TUNEL analysis (Figures S3A and S3B). Among the upregulated negative regulators of cell cycle was the *Cdkn2a* locus, which encodes the G1/S cell-cycle inhibitor INK4A/P16 and a proapoptotic protein, ARF/P19 (Popov and Gil, 2010). qRT-PCR analysis confirmed RNA-seq data and revealed an increase in *Arf* and *Ink4a* expression in the P0 *Ring1a/b* null lingual epithelium compared with control (Figure 3C). ChIP-seq and ChIP-qPCR analyses showed that the *Cdkn2a* locus is marked by H2AK119ub in control lingual epithelial cells (Figures 3D and 3E; Table S3). H2AK119ub marking of the *Cdkn2a* locus was significantly reduced in *Ring1a/b* 2KO lingual epithelium (Figure 3E). To test whether the upregulation of *Cdkn2a* in *Ring1a/b* 2KO directly leads to failure of fungiform papillae and loss of filiform papillae, we ablated *Cdkn2a* in *Ring1a/b* 2KO mice *(Ring1a/b/Cdkn2a* 3KO). The ablation rescued the number of proliferating lingual cells, as shown by analysis of the mitotic-specific marker phospho-histone H3 (PHH3), indicating that the upregulation of the *Cdkn2a* locus contributed to decreased proliferation in *Ring1a/b* null epithelium (Figures 3F and 3G). H&E and IF analyses revealed filiform-like structures in the lingual epithelium of *Ring1a/b/Cdkn2a* 3KO mice (Figure S3G), but not fungiform papillae (Figures 3H and 3I).

In many biological systems, the *Cdkn2a* locus is targeted by PRC2 (Popov and Gil, 2010). Targeting of *Cdkn2a* by the PRC2-dependent H3K27me3 mark in control lingual epithelium was confirmed by ChIP-qPCR (Figure S3C). Although upregulation of *Ink4a* and *Arf* was observed in *Eed* cKO lingual epithelium (Figure S3D), their levels were significantly lower compared with P0 *Ring1a/b* 2KO lingual epithelium (Figure S3D). Analysis of PHH3 showed that proliferation of P0 *Eed* cKO lingual epithelial basal cells was not affected (Figures S3E and S3F), suggesting that ablation of PRC2 alone is not sufficient to cause a reduction in proliferation. Altogether, these data indicate that *Cdkn2a* upregulation in *Ring1a/b* 2KO mice partially contributed to the loss of filiform papillae but did not affect the maintenance of the fungiform papillae.

PRC1 Restricts SHH Signaling in the Non-gustatory Epithelium

We next focused on components of the SHH signaling pathway, shown to be upregulated by our RNA-seq data in *Ring1a/b* 2KO non-gustatory epithelium (Figures 2B and 2C). Using *in situ* hybridization for *Shh* mRNA expression, we found that in contrast to the focal expression of *Shh* mRNA in taste cells within fungiform papillae of control mice (Figures 4A and 4A′), *Shh* mRNA is ectopically expressed in the non-gustatory epithelium of *Ring1a/b* 2KO embryos (Figures 4A and 4A′). Consistent with the ectopic expression of *Shh* in the non-gustatory epithelium of *Ring1a/b* 2KO embryos, *in situ* hybridization analysis of *Gli1* mRNA, a downstream effector of SHH signaling, showed ectopic *Gli1* mRNA expression in the non-gustatory epithelium of E16 *Ring1a/b* 2KO embryos, while in controls, *Gli1* mRNA was limited to the epithelial region and the mesenchymal core of the

developing fungiform papillae (Figures 4B and 4B′). Increased expression of *GIH* was confirmed using a *GIH-LacZ* reporter line (Figure 4C).

During taste cell specification, SHH follows the expression pattern of the WNT pathway, and activation of WNT signaling results in induction of *Shh* expression in the taste cells (Iwatsuki et al., 2007; Liu et al., 2007). To test whether the upregulation of *Shh* mRNA in *Ring1a/b* 2KO non-gustatory epithelium is linked to alterations in WNT signaling, we crossed *Ring1a/b* 2KO mice with the *TCF/Lef:H2B-GFP* reporter line, where histone H2B-GFP fusion protein is expressed under the control of the TCF/LEF responsive element, tracking canonical WNT signaling (Ferrer-Vaquer et al., 2010). We did not detect H2B-GFP in the non-gustatory epithelium of E16 *Ring1a/b* 2KO embryos; H2B-GFP was expressed only in K8(+) taste cells, similar to control embryos (Figure S4A). Furthermore, the expression levels of *Wnt10b*, the activator WNT ligand in the fungiform papillae (Iwatsuki et al., 2007), and *Axin2*, an effector of WNT signaling, in *Ring1a/b* 2KO embryos were similar to control levels at E16 (Figure S4B). These data show that the ectopic expression of *Shh* in the *Ring1a/b* 2KO non-gustatory epithelium does not result from changes in canonical WNT signaling.

To determine whether PRC1 restricts SHH signaling by directly repressing *Shh* expression in the non-gustatory epithetlium, we performed ChIP-seq and ChIP-qPCR analyses of the PRC1-dependent H2AK119ub mark. These analyses revealed that the *Shh* gene is marked by H2AK119ub in control lingual epithelial cells (Figures 4D–4F; Table S3). H2AK119ub marking of the *Shh* locus was significantly reduced in *Fting1a/b* 2KO lingual epithelium (Figures 4E and 4F). We next analyzed the presence of the H2AK119ub mark on *the Shh* locus in FACS-purified taste cells (Figures S4C and S4D), in which *Shh* is robustly expressed. ChIP-qPCR analysis revealed a significant reduction in H2AK119ub marking of the *Shh* locus in taste cells, compared with non-gustatory cells (Figure 4G). Collectively, these findings indicate that PRC1 directly represses *Shh* in the non-gustatory epithelium and that de-repression of *Shh* in the *Ring1a/b* 2KO non-gustatory epithelium results in *Shh* expression and ectopic SHH signaling.

PRC1-Mediated Repression of SHH Signaling in the Non-gustatory Epithelium Is Critical for Fungiform Papillae Maintenance

To test whether ectopic SHH signaling in the non-gustatory epithelium of *Ring1a/b* 2KO mice results in the observed phenotypic alterations, we performed an *in vivo* rescue experiment by ablating *Smo*, a critical downstream effector of SHH (Long et al., 2001), in *Ring1a/b* 2KO mice (*Ring1a/b/Smo* 3KO). *In situ* hybridization confirmed loss of *Gli1* mRNA expression in the lingual epithelium of *Ring1a/b/Smo* 3KO P0 mice, while its expression was detected in mesenchymal cells that are not targeted by *K14-Cre* ablation (Figure 5A). H&E analysis revealed that filiform papillae formation was not rescued in *Ring1a/b/Smo* 3KO mutants (Figure S5). However, K8(+) taste cells, organized in clusters, were detected in *Ring1a/b/Smo* 3KO tongues, although they lacked the organized fungiform papilla shape typical in controls (Figures 5A and 5B). Quantification of K8(+) clusters confirmed that the numbers of K8(+) taste cell clusters were higher in P0 *Ring1a/b/Smo* 3KO tongues compared with P0 *Ring1a/b* 2KO tongues (Figures 5B and 5C). Altogether,

these data show that activation of ectopic SHH signaling in *Ring1a/b* 2KO non-gustatory epithelium results in failure to maintain the fungiform papillae and taste cells.

DISCUSSION

To achieve fully functional tissues, the development and patterning processes have to be precisely regulated, both spatially and temporally. Within the lingual epithelium, patterning of taste cells is essential for the development of a regular array of fungiform papillae and is preceded by spatial changes in expression of genes specific to taste cells (Barlow, 2015; Kapsimali and Barlow, 2013). While the roles of taste cell gene expression in fungiform papillae development have been extensively studied (Barlow, 2015), the mechanisms controlling repression of the taste cell fate in the non-gustatory epithelium and their contribution to fungiform papillae development remain largely unknown.

Here, we identify the PRC1 complex as a regulator of lingual papillae morphogenesis. Our data show that PRC1-mediated repression of *Shh* expression in the non-gustatory epithelium is required for maintenance of the developing fungiform papillae (Figure 5D). We show that ectopic *Shh* expression and activation of SHH signaling in the *Ring1a/b* 2KO non-gustatory epithelium lead to failure of fungiform papillae maintenance, resulting in loss of the papillae and taste cells by birth. Our findings highlight the role of the non-gustatory epithelial cells, contributing to the fungiform papillae structure and filiform papillae, as an essential niche to maintain the integrity of the taste cells through PRC1-mediated inhibition of *Shh* expression.

SHH is a critical morphogen for tongue formation and for taste epithelium specification and patterning (Liu et al., 2004). During E10-E11, *Shh* mRNA is dispersed throughout the single layer of lingual epithelial basal cells (Hall et al., 1999; Iwatsuki et al., 2007). However, as the taste placodes specify, *Shh* transcripts are progressively restricted to the placode, where they are robustly expressed (Thirumangalathu et al., 2009). SHH-negative epithelial cells adjacent to the SHH source evaginate to form the fungiform papillae, while distant cells acquire a non-gustatory fate (Hall et al., 2003). Chemical inhibition and genetic ablation of SHH signaling during taste cell specification and early fungiform papillae development (E12.5–E14.5) result in formation of ectopic and enlarged fungiform papillae, whereas induction of ectopic SHH at these time points has been shown to inhibit fungiform papillae formation (El Shahawy et al., 2017; Hall et al., 2003; Iwatsuki et al., 2007; Mistretta et al., 2003). Although inhibition of endogenous SHH signaling later than E14.5, after the pattern of fungiform papillae has been established, does not alter this pre-existing pattern or fungiform papillae size (Liu et al., 2004), the outcome of ectopic activation of SHH signaling after the fungiform papillae pattern is established remains unknown. Our studies show that *Shh* is ectopically expressed in *Ring1a/b* 2KO non-gustatory epithelium, resulting in ectopic SHH signaling and collapse of fungiform papillae. Ablation of *Smo* in *Ring1a/b* 2KO tongues partially rescued the maintenance of taste cells, signifying that consistent repression of *Shh* in non-gustatory cells is critical to maintain the taste cell cluster integrity.

The lingual phenotype of *Ring1a/b* 2KO is complex. Fungiform papillae with taste cell clusters develop normally and then gradually collapse, and filiform papillae fail to develop. Proper initiation of fungiform papillae development is expected, because the PRC1-

dependent H2AK119ub mark is lost in *Ring1a/b* 2KO tongues only at E16.5, when a pattern of fungiform papillae is already established. Therefore, the role of PRC1 in early patterning of fungiform papillae remains an open question. In contrast, filiform papillae develop between E17.5 and E18, after the H2AK119ub mark is lost in *Ring1a/b* 2KO tongues. This allows us to determine that PRC1 is essential for filiform papillae formation. While the rescue of taste cell clusters seen in *Ring1a/b/Smo* 3KO emphasizes the role of *Shh* repression in the non-gustatory niche in taste cell maintenance, the failure to rescue the filiform papillae and the fungiform papillae shape indicate that SHH signaling may interact with additional pathways to maintain the structure of the fungiform papillae niche. Ablation of PRC1, a global epigenetic regulator, has led to significant alterations in gene expression, as shown by RNA-seq analysis. Those changes may be direct, as in the case of *Shh* and *Cdkn2a,* or indirect. The downregulated genes in *Ring1a/b* 2KO tongues may shed light on the additional mechanisms of PRC1 regulation in the lingual epithelium. Loss of lingual keratinocyte identity, evident by the downregulation of genes such as *Krt6a, Krt6b, Krt13,* and *Pax9,* may explain why the structures of fungiform and filiform papillae are disrupted in *Ring1a/b* 2KO tongues. Given the growing evidence that PRC1 also promotes gene expression (Chan et al., 2018; Cohen et al., 2018, 2019; Gao et al., 2014), it is intriguing to hypothesize that a similar role for PRC1 in promoting lingual keratinocyte genes is responsible for some observed phenotypes in *Ring1a/b* 2KO tongues.

Our studies show that PRC1 is important for lingual papillae formation, while PRC2 is dispensable. Based on biochemical studies, it has been assumed that these two complexes cotarget the same genes (Margueron and Reinberg, 2011). Genetic studies in *Drosophila* showed that loss of PRC1 or PRC2 core subunits results in similar homeotic transformations, supporting the model that two complexes function together (Lanzuolo and Orlando, 2012). However, our genetic studies of lingual epithelium show that the current model of Polycomb-mediated gene control may be too simplistic. While both PRC1 and PRC2 are functional in the lingual epithelium, only loss of PRC1 results in ablation of lingual papillae. Loss of PRC2 results in apparently normal lingual epithelium, and ablation of both complexes produces a phenotype similar to that of PRC1 ablation. These findings indicate that PRC1 repression in the non-gustatory epithelium plays a role in the development of the lingual papillae, while PRC2 is dispensable.

Our studies establish a critical role for PRC1 in the development of lingual papillae and may pave the way for evaluating the role of PRC1 in regeneration of adult lingual epithelium and in oral diseases, including cancer. PRC1's subunit BMI1 has been shown to broadly label the oral epithelial basal cells of adult mice (Jones et al., 2019; Tanaka et al., 2013) and serve as a biomarker of cancer stem cells (Tanaka et al., 2016). However, it is unknown whether PRC1-BMI1 complexes are functionally important in adult lingual epithelium and oral cancer. Furthermore, understanding the molecular pathways behind the patterning of the tongue and taste system may have broader implications for various lingual pathologies, including congenital taste disorders and drug-related alterations in taste sensation. Specifically, basal cell carcinoma patients, treated with inhibitors of the SHH pathway, which is critical for taste sensation in adults (Kumari et al., 2015, 2017), experience severe taste disturbances (LoRusso et al., 2011; Rodon et al., 2014; Tang et al., 2012), causing an adverse effect on their quality of life (Lacouture et al., 2016).

STAR★METHODS

LEAD CONTACT AND MATERIALS AVAILABILITY

Further information and requests for resources and reagents should be directed to and be fulfilled by the Lead Contact, Dr. Elena Ezhkova (elena.ezhkova@mssm.edu).

EXPERIMENTAL MODEL AND SUBJECT DETAILS

All mice used for this study were housed at the Center of Comparative Medicine and Surgery (CCMS), Icahn School of Medicine at Mount Sinai (ISMMS), according to the Institutional Animal Care and Use Committee (IACUC) guidelines (Protocol number LA11-0020). *Krt14-Cre, Smo^flox/flox^, Gli1^lacZ^, TCF/Lef:H2B-GFP* and *Rosa26-mT/mG* mice were obtained from the Jackson Laboratories. *Eed^flox/flox^* mice were kindly provided by Weipeng Mu and Terry Magnuson (Mu et al., 2014). *Ink4a/Arf^−/−^* mice were kindly provided by Philippe Soriano (Serrano et al., 1996). Both male and female mice were used in this study. Primer sequences used for genotyping are available in Table S4. BrdU was administered to newborn P0 mice by sub-cutaneous injection (50μg per 1g of mouse weight) 4 hours before sacrifice.

METHOD DETAILS

No randomization or blinding was performed in this study. Sample size is indicated in figure legends and statistical methods are indicated in the quantification and statistical analysis paragraph.

Fluorescence-activated cell sorting—Basal lingual epithelial cells were purified from E16 embryos and P0 newborn mice. Tongues were removed from the mandible and cut to exclude the posterior circumvallate papillae (CV). For RNA and RNA-Seq analysis of control, *Krt14-Cre Ring1a^−/−^ Ring1b^flox/flox^* mice, E16 tongues were collected. For analysis of control and *Krt14-Cre Eed^flox/flox^* mice, P0 tongues were collected. For taste cell isolation, P0 tongues from P0 TCF/LEF:H2B-GFP(+) mice were collected. Tissues were cut into small pieces and incubated with 1.26U/mL dispase (Invitrogen) and 0.3% type 1 collagenase (Worthington) for one hour at 37°C with 80 rpm shaking. Tissues were washed with 1x PBS, dissociated with 0.25% Trypsin with 2.21mM EDTA (Corning Cellgro; Manassas, VA, USA), and then washed twice with 1xPBS. Cells were stained with 1:400 EpCAM-APC antibodies (Biolegend; San Diego, CA, USA) for 30 min on ice and washed twice with 1x HBSS prior to cell sorting. For ChIP analysis, control, *Ring1a/b* 2KO, and TCF/LEF:H2B-GFP (+) newborn P0 mice were collected. All cell isolations were performed on a FACS BD Influx or BD FACSAria II instruments (BD, Franklin Lakes, NJ, USA) at the Flow Cytometry Core Facility at Icahn School of Medicine at Mount Sinai.

Chromatin Immunoprecipitation, ChIP-qPCR and Library preparation—
Chromatin immunoprecipitation (ChIP) was performed on FACS-sorted populations using materials and methods as previously described (Lien et al., 2011). A total of 0.5×10^6 cells was used for H2AK119ub per replicate, for ChIP-seq and qPCR validations. 5×10^4 cells were used for ChIP-qPCR on *Krt14-Cre Ring1a^−/−^ Ring1b^flox/flox^* mice and 2.5×10^4 cells were used for ChIP-qPCR on TCF/LEF:H2B-GFP(+) taste cells. Prior to cell sorting, cells

were stained for viability using Zombie Violet (Biolegend; San Diego, CA), then cross-linked using fresh solution with a final concentration of 1% formaldehyde (Thermo Fisher Scientific; Rockford, IL) for 10 minutes on ice. Crosslinking was stopped by the addition of Glycine (final concentration 125mM) for 5 minutes of incubation at room temperature, followed by two washes with 1x PBS. Cells were incubated in lysis buffer 1 (50mM HEPES pH = 7.5, 140mM NaCl, 1mM EDTA, 10% glycerol, 0.5% NP-40, 0.25% Triton X-100, protease inhibitor cocktail (Roche) for 10 min on ice, then incubated for 10 min with lysis buffer 2 (10mM Tris-HCl pH = 7.5, 200mM NaCl, 1mM EDTA, 0.5mM EGTA). Before ChIP, cells were resuspended in lysis buffer 3 (10mM Tris-HCl pH = 8.0, 200mM NaCl, 1mM EDTA, 0.5mM EGTA, 0.1% Na-deoxycholate, 0.5% N-laurylsarcosine, 1% Triton X-100) and sonicated using a Branson Sonifier at 25% power output for 15 cycles of 30 s of sonication followed by 90 s of rest in an ice bath. Chromatin was incubated overnight at 4°C with antibodies as indicated in Table S4. Dynal protein G magnetic beads (Invitrogen) were added the next day and incubated for 6 hours. The beads were sequentially washed with low salt, high salt, LiCl, and Tris-EDTA buffers for 10 minutes each at 4°C. Bound chromatin was eluted, and crosslinking was reversed by overnight incubation at 65°C, followed by RNase A (Sigma-Aldrich) and proteinase K (Roche Diagnostics) treatments. Samples were purified using ChIP DNA Clean and Concentrator kit (Zymo Research; Irvine, CA). Samples were analyzed by qPCR using LightCycler® 480 SYBR Green I Master Mix (Roche Diagnostics) on a Lightcycler 480 instrument (Roche). Primer sequences are available in Table S4. For high-throughput ChIP sequencing, libraries were constructed from 4ng of Purified DNA using the DNA SMART ChIP-Seq Kit (Clontech; Palo Alto, CA, USA) according to the manufacturer's instructions. Constructed ChIP-seq libraries were sequenced (75-bp single ended) by the Tisch Cancer Center sequencing facility at ISMMS, on the Illumina NextSeq 500 platform. Two biological replicates were used for ChIP experiments.

RNA purification, RT-qPCR, and RNA-seq library preparation—FACS-purified cells were collected directly into RLT Plus buffer (QIAGEN), and total RNA was isolated with the RNeasy Plus Micro Kit (QIAGEN). Complimentary DNA was reverse-transcribed from total RNA using qScript cDNA SuperMix (Quanta Biosciences, Gaithersburg, MD, USA) according to the manufacturer's instructions. Samples were analyzed by RT-qPCR using LightCycler® 480 SYBR Green I Master Mix (Roche Diagnostics) on a Lightcycler 480 instrument (Roche). Results were normalized to *Ppib* mRNA levels. Primer sequences are available in Table S4. Prior to library construction, sample quality was measured using an Agilent Bioanalyzer, and samples with RNA integrity numbers > 8 were used. 15ng of RNA were reverse transcribed and amplified using the Ovation RNA-seq System V2 (Nugen). Libraries were constructed from 50ng of sonicated cDNA (Covaris) using the Ovation Ultra Low DR Multiplex system (Nugen). The concentration and quality of the libraries were determined using Qubit (Invitrogen) and Bioanalyzer (Agilent). Constructed RNA-seq libraries were sequenced at GENEWIZ on the Illumina HiSeq platform, obtaining 150 nucleotide paired-end reads.

Immunofluorescence, β-galactosidase detection, *in situ* hybridization and imaging—Tongue tissues with underlying mandible were collected from mice, embedded

in OCT compound (Tissue-Tek, Torrance, CA, USA), without prior fixation, in sagittal orientation. Tissues were subsequently cut into 7-8 μm sections using a Leica Cryostat. Slides were then pre-fixed in 4% PFA for 10 minutes at room temperature and blocked overnight at 4°C in blocking solution (1x PBS supplemented with 0.1% Triton X-100,1% BSA, 0.25% normal donkey serum, 0.01% gelatin). Primary antibodies were diluted in blocking solution and incubated for 1 hour, followed by 1-hour incubation with secondary antibodies. Slides were counterstained with DAPI to visualize nuclei. TUNEL apoptosis detection assay was performed using the *in situ* Cell Death Detection Kit, Fluorescein (Roche), according to manufacturer's instructions. β-Galactosidase detection assay was performed on sections fixed for 2 minutes in 0.5% glutaraldehyde (Electron Microscopy Sciences), washed with IxPBS and incubated with 1 mg/ml X-gal substrate in PBS with 1.3 mM $MgCl_2$, 3 mM $K_3Fe(CN)_6$, and 3 mM $K_4Fe(CN)_6$ for three hours at 37°C. Nuclei were counterstained with Fast Red solution (RICCAA). *In situ* hybridization for *Shh* and *Gli1* was performed using RNAscope probes and 2.5HD-RED detection kit (Advanced Cell Diagnostics), according to manufacturer's protocol. All slides were imaged using a Leica DM5500 slide microscope using 20x objectives.

Scanning Electron Microscopy—Tongue tissues with underlying mandible were collected and fixed overnight in 3% glutaraldehyde with 0.2M sodium cacodylate buffer overnight. Tissues were treated with 1% Osmium tetroxide for one hour and dehydrated in increasing Ethanol concentrations and critical-point dried with liquid carbon dioxide. Tissues were then sputter-coated with gold palladium and looked in. Samples were imaged using a Hitachi S4300 scanning electron microscope. All steps of tissue processing and imaging were performed at the Electron Microscopy Core at ISMMS.

QUANTIFICATION AND STATISTICAL ANALYSIS

Quantification of BrdU(+) cells and Phospho-Histone H3(+) cells for cell proliferation analysis—For proliferation analysis, BrdU(+) and Phospho-Histone H3(+) (PHH3) cells in the basal lingual epithelium were quantified using the Leica LASAF software. Nuclear DAPI staining was used to count the total number of cells in the basal layer, and the data are shown as the percentage of BrdU(+) or PHH3(+) cells in the basal layer. At least 40 random and non-overlapping tongue regions, spanning the tongue length were used for quantification in each animal group, from at least two animals of at least two independent litters (n ≥ 2). Comparisons and statistics were performed between matching knockout and control littermates. number of animals used for analysis is indicated in figure legends.

Quantification of KRT8(+) Taste Cell Clusters—For quantification of fungiform papillae, taste cell clusters were defined as groups of adjacent cells and were quantified by the number of K8(+) clusters per millimeter (mm) of tongue. Clusters where cells appeared clearly separated or single cells were not quantified. Sections had typical tongue length ranging between 4-6 mm. At least 100 mm of total tongue length were analyzed per animal, and the average count of a single animal was considered a single data point. At least two animals (n ≥ 2) from at least two independent litters were used for analysis. Comparisons

and statistics were performed between matching knockout and control littermates. The number of animals used for analysis is indicated in figure legends.

ChIP-seq analysis and Data visualization—ChIP-seq reads were aligned to the mm10 reference genome using bowtie2 (v2.3.3, default parameters). Duplicate reads were removed by the Samtools software v0.1.19 (Li et al., 2009). Peaks (mostly broad) in H2AK119ub1 ChIP samples were called as previously described (Goldberg et al., 2010) for the two replicates independently. The peaks were associated to genes as described previously (Cohen et al., 2018) and are provided in Table S3. To visualize ChIP-seq signals, we used the Integrative Genomics Viewer (IGV; http://software.broadinstitute.org/software/igv/) and TDF files from the igvtools (v2.3.57; https://software.broadinstitute.org/software/igv/igvtools).

RNA-seq analysis and data visualization—RNA-seq reads were aligned to the mouse reference genome (mm10) using Tophat (v2.0.13; https://ccb.jhu.edu/software/tophat/index.shtml) gene models of Refgene were downloaded from the UCSC genome browser on March 13, 2017. FPKM (Fragments Per Kilobase of transcript per Million mapped reads) values were generated using cufflinks (v2.2.1; http://cole-trapnell-lab.github.io/cufflinks/). Lowly expressed genes (mean FPKM values < 1 in both groups under comparison) were excluded from differential expression analysis. We analyzed read counts from the HTSeq (v0.6.1;https://github.com/simon-anders/htseq) for differential analysis, using the DESeq2 v1.6.3 (Love et al., 2014), and considered genes with Log2 (fold change) 1.8 and false discovery rate (FDR) < 0.05 as significantly differentially expressed. The list of differentially expressed genes is provided in Table S1.

Gene Ontology enrichment analysis—Identification of significantly over-represented functional categories was done using DAVID Selected GO terms were considered significant with $p < 0.05$ and are shown in Figures 2B, 2E and Table S2.

Statistics—To determine the statistical significance between two groups, two-sided t tests were performed. Mann-Whitney test was performed when Gaussian distribution could not be assumed. To determine the statistical significance between more than two groups, where all subjects within a group carry the same genotype, comparisons were made using one-way ANOVA with the Bonferroni post hoc test. Kruskal-Wallis test and Dunn's post-test were performed when Gaussian distribution could not be assumed.

Scatter dot plots error bars represent the mean with SEM. Scatter on a bar graph plots data points represent the average measure of distinct biological replicates and the bar represents the average of all replicates. Error bars represent the mean ± SEM. All data in bar graphs are presented as mean ± SEM, except Figure 3C, that are mean ± SD. The number of biological replicates used for comparison is indicated in each figure. For each comparison, at least 2 animals for each group from at least two independent litters were used (n 2). Significance levels were defined as *$p < 0.05$; **$p < 0.01$; ***$p < 0.001$; NS, not significant. GraphPad Prism 8 software was used for statistical analyses.

DATA AND CODE AVAILABILITY

The accession number for RNA-seq and ChIP-seq datasets reported in this paper is NCBI GEO: GSE123095.

Supplementary Material

Refer to Web version on PubMed Central for supplementary material.

ACKNOWLEDGMENTS

REFERENCES

Anders S, Pyl PT, and Huber W (2015). HTSeq-a Python framework to work with high-throughput sequencing data. Bioinformatics 31, 166–169. [PubMed: 25260700]

Barlow LA (2015). Progress and renewal in gustation: new insights intotaste bud development. Development 142, 3620–3629. [PubMed: 26534983]

Barlow LA, and Klein OD (2015). Developing and regenerating a sense of taste. Curr. Top. Dev. Biol 111, 401–419. [PubMed: 25662267]

Biggs LC, and Mikkola ML (2014). Early inductive events in ectodermal appendage morphogenesis. Semin. Cell Dev. Biol 25–26, 11–21.

Boyer LA, Plath K, Zeitlinger J, Brambrink T, Medeiros LA, Lee TI, Levine SS, Wernig M, Tajonar A, Ray MK, et al. (2006). Polycomb complexes repress developmental regulators in murine embryonic stem cells. Nature 447, 349–353.

Bracken AP, and Helin K (2009). Polycomb group proteins: navigators of lineage pathways led astray in cancer. Nat. Rev. Cancer 9, 773–784. [PubMed: 19851313]

Cales C, Roman-Trufero M, Pavon L, Serrano I, Melgar T, Endoh M, Perez C, Koseki H, and Vidal M (2008). Inactivation of the polycomb group protein Ring1B unveilsan antiproliferative role in hematopoietic cell expansion and cooperation with tumorigenesis associated with Ink4a deletion. Mol. Cell Biol 28, 1018–1028. [PubMed: 18039844]

Cao R, and Zhang Y (2004). SUZ12 is required for both the histone methyltransferase activity and the silencing function ofthe EED-EZH2 complex. Mol. Cell 75, 57–67.

Cao R, Wang L, Wang H, Xia L, Erdjument-Bromage H, Tempst P, Jones RS, and Zhang Y (2002). Role of histone H3 lysine 27 methylation in Polycomb-group silencing. Science 298, 1039–1043. [PubMed: 12351676]

Chan HL, Beckedorff F, Zhang Y, Garcia-Huidobro J, Jiang H, Colaprico A, Bilbao D, Figueroa ME, LaCava J, Shiekhattar R, and Morey L (2018). Polycomb complexes associate with enhancers and promote oncogenic transcriptional programs in cancer through multiple mechanisms. Nat. Commun 9, 3377. [PubMed: 30139998]

Chiacchiera F, Rossi A, Jammula S, Piunti A, Scelfo A, Ordonez-Moran P, Huelsken J, Koseki H, and Pasini D (2016). Polycomb Complex PRC1 Preserves Intestinal Stem Cell Identity by Sustaining Wnt/b-Catenin Transcriptional Activity. Cell Stem Cell 78, 91–103.

Cohen I, Zhao D, Bar C, Valdes VJ, Dauber-Decker KL, Nguyen MB, Nakayama M, Rendl M, Bickmore WA, Koseki H, et al. (2018). PRC1 Fine-tunes Gene Repression and Activation to

Safeguard Skin Development and Stem Cell Specification. Cell Stem Cell 22, 726–739. [PubMed: 29727681]

Cohen I, Zhao D, Menon G, Nakayama M, Koseki H, Zheng D, and Ezhkova E (2019). PRC1 preserves epidermal tissue integrity independently of PRC2. Genes Dev. 88, 55–60.

Dauber KL, Perdigoto CN, Valdes VJ, Santoriello FJ, Cohen I, and Ezhkova E (2016). Dissecting the roles of polycomb repressive complex 2 subunits in the control of skin development. J. Invest. Dermatol 786, 1647–1655.

de Napoles M, Mermoud JE, Wakao R, Tang YA, Endoh M, Appanah R, Nesterova TB, Silva J, Otte AP, Vidal M, et al. (2004). Polycomb group proteins Ring1A/B link ubiquitylation of histone H2A to heritable gene silencing and X inactivation. Dev. Cell 7, 663–676. [PubMed: 15525528]

del Mar Lorente M, Marcos-Gutierrez C, Perez C, Schoorlemmer J, Ram-irez A, Magin T, and Vidal M (2000). Loss- and gain-of-function mutations show a polycomb group function for Ring1A in mice. Development 727, 5093–5100.

El Shahawy M, Reibring CG, Neben CL, Hallberg K, Marangoni P, Harfe BD, Klein OD, Linde A, and Gritli-Linde A (2017). Cell fate specification in the lingual epithelium is controlled by antagonistic activities of Sonic hedgehog and retinoic acid. PLoS Genet. 78, e1006914.

Endoh M, Endo TA, Endoh T, Isono K, Sharif J, Ohara O, Toyoda T, Ito T, Eskeland R, Bickmore WA, et al. (2012). Histone H2A mono-ubiquitination is a crucial step to mediate PRC1-dependent repression of developmental genes to maintain ES cell identity. PLoS Genet. 8, e1002774. [PubMed: 22844243]

Endoh M, Endo TA, Shinga J, Hayashi K, Farcas A, Ma KW, Ito S, Sharif J, Endoh T, Onaga N, et al. (2017a). PCGF6-PRC1 suppresses premature differentiation of mouse embryonic stem cells by regulating germ cell-related genes. eLife 6, e21064. [PubMed: 28304275]

Endoh M, Endo TA, Shinga J, Hayashi K, Farcas A, Ma KW, Ito S, Sharif J, Endoh T, Onaga N, et al. (2017b). Correction: PCGF6-PRC1 suppresses premature differentiation of mouse embryonic stem cells by regulating germ cell-related genes. eLife 6, e27970. [PubMed: 28440749]

Ezhkova E, Pasolli HA, Parker JS, Stokes N, Su IH, Hannon G, Tarakhovsky A, and Fuchs E (2009). Ezh2 orchestrates gene expression for the stepwise differentiation of tissue-specific stem cells. Cell 786, 1122–1135.

Faust C, Schumacher A, Holdener B, and Magnuson T (1995). The eed mutation disrupts anterior mesoderm production in mice. Development 727, 273–285.

Ferrer-Vaquer A, Piliszek A, Tian G, Aho RJ, Dufort D, and Hadjantonakis AK (2010). A sensitive and bright single-cell resolution live imaging reporter of Wnt/8-catenin signaling in the mouse. BMC Dev. Biol 70, 121.

Gao Z, Zhang J, Bonasio R, Strino F, Sawai A, Parisi F, Kluger Y, and Reinberg D (2012). PCGF homologs, CBX proteins, and RYBP define functionally distinct PRC1 family complexes. Mol. Cell 45, 344–356. [PubMed: 22325352]

Gao Z, Lee P, Stafford JM, von Schimmelmann M, Schaefer A, and Reinberg D (2014). An AUTS2-Polycomb complex activates gene expression in the CNS. Nature 576, 349–354.

Goldberg AD, Banaszynski LA, Noh K-M, Lewis PW, Elsaesser SJ, Stadler S, Dewell S, Law M, Guo X, Li X, et al. (2010). Distinct factors control histone variant H3.3 localization at specific genomic regions. Cell 740,678–691.

Hall JM, Hooper JE, and Finger TE (1999). Expression of sonic hedge-hog, patched, and Gli1 in developing taste papillae of the mouse. J. Comp. Neurol 406, 143–155. [PubMed: 10096602]

Hall JM, Bell ML, and Finger TE (2003). Disruption of sonic hedgehog signaling alters growth and patterning of lingual taste papillae. Dev. Biol 255,263–277. [PubMed: 12648489]

Huang da W, Sherman BT, and Lempicki RA (2009). Systematic and integrative analysis of large gene lists using DAVID bioinformatics resources. Nat. Protoc 4, 44–57. [PubMed: 19131956]

Iwasaki S, Yoshizawa H, and Aoyagi H (2006). Immunohistochemical expression of keratins 13 and 14 in the lingual epithelium of rats during the morphogenesis of filiform papillae. Arch. Oral Biol 57, 416–426.

Iwatsuki K, Liu HX, Gronder A, Singer MA, Lane TF, Grosschedl R, Mistretta CM, and Margolskee RF (2007). Wnt signaling interacts with Shh to regulate taste papilla development. Proc. Natl. Acad. Sci. USA 704, 2253–2258.

Jones KB, Furukawa S, Marangoni P, Ma H, Pinkard H, D'Urso R, Zilionis R, Klein AM, and Klein OD (2019). Quantitative Clonal Analysis and Single-Cell Transcriptomics Reveal Division Kinetics, Hierarchy, and Fate of Oral Epithelial Progenitor Cells. Cell Stem Cell 24, 183–192. [PubMed: 30472156]

Jonker L, Kist R, Aw A, Wappler I, and Peters H (2004). Pax9 is required for filiform papilla development and suppresses skin-specific differentiation of the mammalian tongue epithelium. Mech. Dev 727, 1313–1322.

Juan AH, Derfoul A, Feng X, Ryall JG, Dell'Orso S, Pasut A, Zare H, Simone JM, Rudnicki MA, and Sartorelli V (2011). Polycomb EZH2 controls self-renewal and safeguards the transcriptional identity of skeletal muscle stem cells. Genes Dev. 25, 789–794. [PubMed: 21498568]

Kallin EM, Cao R, Jothi R, Xia K, Cui K, Zhao K, and Zhang Y (2009). Genome-wide uH2A localization analysis highlights Bmi1-dependent deposition ofthe mark at repressed genes. PLoS Genet. 5, e1000506. [PubMed: 19503595]

Kapsimali M, and Barlow LA (2013). Developing a sense of taste. Semin. Cell Dev. Biol 24, 200–209.

Ketel CS, Andersen EF, Vargas ML, Suh J, Strome S, and Simon JA (2005). Subunit contributions to histone methyltransferase activities of fly and worm polycomb group complexes. Mol. Cell. Biol 25, 6857–6868. [PubMed: 16055700]

Kumari A, Ermilov AN, Allen BL, Bradley RM, Dlugosz AA, and Mistretta CM (2015). Hedgehog pathway blockade with the cancer drug LDE225 disrupts taste organs and taste sensation. J. Neurophysiol 778, 1034–1040.

Kumari A, Ermilov AN, Grachtchouk M, Diugosz AA, Allen BL, Bradley RM, and Mistretta CM (2017). Recovery of taste organs and sensory function after severe loss from Hedgehog/ Smoothened inhibition with cancer drug sonidegib. Proc. Natl. Acad. Sci. USA 114, E10369–E10378. [PubMed: 29133390]

Lacouture ME, Dreno B, Ascierto PA, Dummer R, Basset-Seguin N, Fife K, Ernst S, Licitra L, Neves RI, Peris K, et al. (2016). Characterization and Management of Hedgehog Pathway Inhibitor-Related Adverse Events in Patients With Advanced Basal Cell Carcinoma. Oncologist 21, 1218–1229. [PubMed: 27511905]

Lanzuolo C, and Orlando V (2012). Memories from the polycomb group proteins. Annu. Rev. Genet 46, 561–589. [PubMed: 22994356]

Lessard JC, and Coulombe PA (2012). Keratin 16-null mice develop palmoplantar keratoderma, a hallmark feature of pachyonychia congenita and related disorders. J. Invest. Dermatol 132, 1384–1391. [PubMed: 22336941]

Li H, Handsaker B, Wysoker A, Fennell T, Ruan J, Homer N, Marth G, Abecasis G, and Durbin R; 1000 Genome Project Data Processing Sub-group (2009). The Sequence Alignment/Map format and SAMtools. Bioinformatics 25,2078–2079.

Lien WH, Guo X, Polak L, Lawton LN, Young RA, Zheng D, and Fuchs E (2011). Genome-wide maps of histone modifications unwind in vivo chromatin states of the hair follicle lineage. Cell Stem Cell 9, 219–232. [PubMed: 21885018]

Liu HX, Maccallum DK, Edwards C, Gaffield W, and Mistretta CM (2004). Sonic hedgehog exerts distinct, stage-specific effects on tongue and taste papilla development. Dev. Biol 276, 280–300. [PubMed: 15581865]

Liu F, Thirumangalathu S, Gallant NM, Yang SH, Stoick-Cooper CL, Reddy ST, Andl T, Taketo MM, Dlugosz AA, Moon RT, et al. (2007). Wnt-beta-catenin signaling initiates taste papilla development. Nat. Genet 39, 106–112. [PubMed: 17128274]

Long F, Zhang XM, Karp S, Yang Y, and McMahon AP (2001). Genetic manipulation of hedgehog signaling in the endochondral skeleton reveals a direct role in the regulation of chondrocyte proliferation. Development 128, 5099–5108. [PubMed: 11748145]

LoRusso PM, Rudin CM, Reddy JC, Tibes R, Weiss GJ, Borad MJ, Hann CL, Brahmer JR, Chang I, Darbonne WC, et al. (2011). Phase I trial of hedgehog pathway inhibitor vismodegib (GDC-0449) in patients with refractory, locally advanced or metastatic solid tumors. Clin. Cancer Res 17,2502–2511. [PubMed: 21300762]

Love MI, Huber W, and Anders S (2014). Moderated estimation of fold change and dispersion for RNA-seq data with DESeq2. Genome Biol. 15, 550. [PubMed: 25516281]

Ma L, Lopez GF, and Krimm RF (2009). Epithelial-derived brain-derived neurotrophic factor is required for gustatory neuron targeting during a critical developmental period. J. Neurosci 29, 3354–3364. [PubMed: 19295142]

Manabe M, Lim HW, Winzer M, and Loomis CA (1999). Architectural organization of filiform papillae in normal and black hairy tongue epithelium: dissection of differentiation pathways in a complex human epithelium according to their patterns of keratin expression. Arch. Dermatol 135, 177–181. [PubMed: 10052403]

Margueron R, and Reinberg D (2011). The Polycomb complex PRC2 and its mark in life. Nature 469, 343–349. [PubMed: 21248841]

Mbiene JP, and Roberts JD (2003). Distribution of keratin 8-containing cell clusters in mouse embryonic tongue: evidence for a prepattern for taste bud development. J. Comp. Neurol 457, 111–122. [PubMed: 12541313]

Min J, Zhang Y, and Xu RM (2003). Structural basis for specific binding of Polycomb chromodomain to histone H3 methylated at Lys 27. Genes Dev. 17, 1823–1828. [PubMed: 12897052]

Misra M, Audoly B, and Shvartsman SY (2017). Complex structures from patterned cell sheets. Philos. Trans. R. Soc. Lond. B Biol. Sci 372, 20150515. [PubMed: 28348251]

Mistretta CM, and Kumari A (2017). Tongue and Taste Organ Biology and Function: Homeostasis Maintained by Hedgehog Signaling. Annu. Rev. Physiol 79, 335–356. [PubMed: 28192057]

Mistretta CM, Liu HX, Gaffield W, and MacCallum DK (2003). Cyclopamine and jervine in embryonic rat tongue cultures demonstrate a role for Shh signaling in taste papilla development and patterning: fungiform papillae double in number and form in novel locations in dorsal lingual epithelium. Dev. Biol 254, 1–18. [PubMed: 12606278]

Mu W, Starmer J, Fedoriw AM, Yee D, and Magnuson T (2014). Repression of the soma-specific transcriptome by Polycomb-repressive complex 2 promotes male germ cell development. Genes Dev. 28, 2056–2069. [PubMed: 25228648]

Muzumdar MD, Tasic B, Miyamichi K, Li L, and Luo L (2007). A global double-fluorescent Cre reporter mouse. Genesis 45, 593–605. [PubMed: 17868096]

Okubo T, Pevny LH, and Hogan BL (2006). Sox2 is required for development of taste bud sensory cells. Genes Dev. 20, 2654–2659. [PubMed: 17015430]

Pasini D, Bracken AP, Jensen MR, Lazzerini Denchi E, and Helin K (2004). Suz12 is essential for mouse development and for EZH2 histone methyltransferase activity. EMBO J. 23, 4061–4071. [PubMed: 15385962]

Popov N, and Gil J (2010). Epigenetic regulation of the INK4b-ARF-INK4a locus: in sickness and in health. Epigenetics 5, 685–690. [PubMed: 20716961]

Rodon J, Tawbi HA, Thomas AL, Stoller RG,Turtschi CP, Baselga J, Sarantopoulos J, Mahalingam D, Shou Y, Moles MA, et al. (2014). A phase I, multicenter, open-label, first-in-human, dose-escalation study of the oral smoothened inhibitor Sonidegib (LDE225) in patients with advanced solid tumors. Clin. Cancer Res 20, 1900–1909. [PubMed: 24523439]

Rothnagel JA, Seki T, Ogo M, Longley MA, Wojcik SM, Bundman S, Bickenbach JR, and Roop DR (1999). The mouse keratin 6 isoforms are differentially expressed in the hair follicle, footpad, tongue and activated epidermis. Differentiation 65, 119–130. [PubMed: 10550545]

Serrano M, Lee H, Chin L, Cordon-Cardo C, Beach D, and DePinho RA (1996). Role of the INK4a locus in tumor suppression and cell mortality. Cell 85, 27–37. [PubMed: 8620534]

Simon JA, and Kingston RE (2009). Mechanisms of polycomb gene silencing: knowns and unknowns. Nat. Rev. Mol. Cell Biol 10, 697–708. [PubMed: 19738629]

Simon JA, and Kingston RE (2013). Occupying chromatin: Polycomb mechanisms for getting to genomic targets, stopping transcriptional traffic, and staying put. Mol. Cell 49, 808–824. [PubMed: 23473600]

Simon J, Chiang A, and Bender W (1992). Ten different Polycomb group genes are required for spatial control of the abdA and AbdB homeotic products. Development 114, 493–505. [PubMed: 1350533]

Tanaka T, Komai Y, Tokuyama Y, Yanai H, Ohe S, Okazaki K, and Ueno H (2013). Identification of stem cells that maintain and regenerate lingual keratinized epithelial cells. Nat. Cell Biol 15, 511–518. [PubMed: 23563490]

Tanaka T, Atsumi N, Nakamura N, Yanai H, Komai Y, Omachi T, Tanaka K, Ishigaki K, Saiga K, Ohsugi H, et al. (2016). Bmi1-positive cells in the lingual epithelium could serve as cancer stem cells in tongue cancer. Sci. Rep 6, 39386. [PubMed: 28004815]

Tang JY, Mackay-Wiggan JM, Aszterbaum M, Yauch RL, Lindgren J, Chang K, Coppola C, Chanana AM, Marji J, Bickers DR, and Epstein H Jr. (2012). Inhibiting the hedgehog pathway in patients with the basal-cell nevus syndrome. N. Engl. J. Med 366, 2180–2188. [PubMed: 22670904]

Thirumangalathu S, Harlow DE, Driskell AL, Krimm RF, and Barlow LA (2009). Fate mapping of mammalian embryonic taste bud progenitors. Development 136, 1519–1528. [PubMed: 19363153]

Wang H, Wang L, Erdjument-Bromage H, Vidal M, Tempst P, Jones RS, and Zhang Y (2004). Role of histone H2A ubiquitination in Polycomb silencing. Nature 431, 873–878. [PubMed: 15386022]
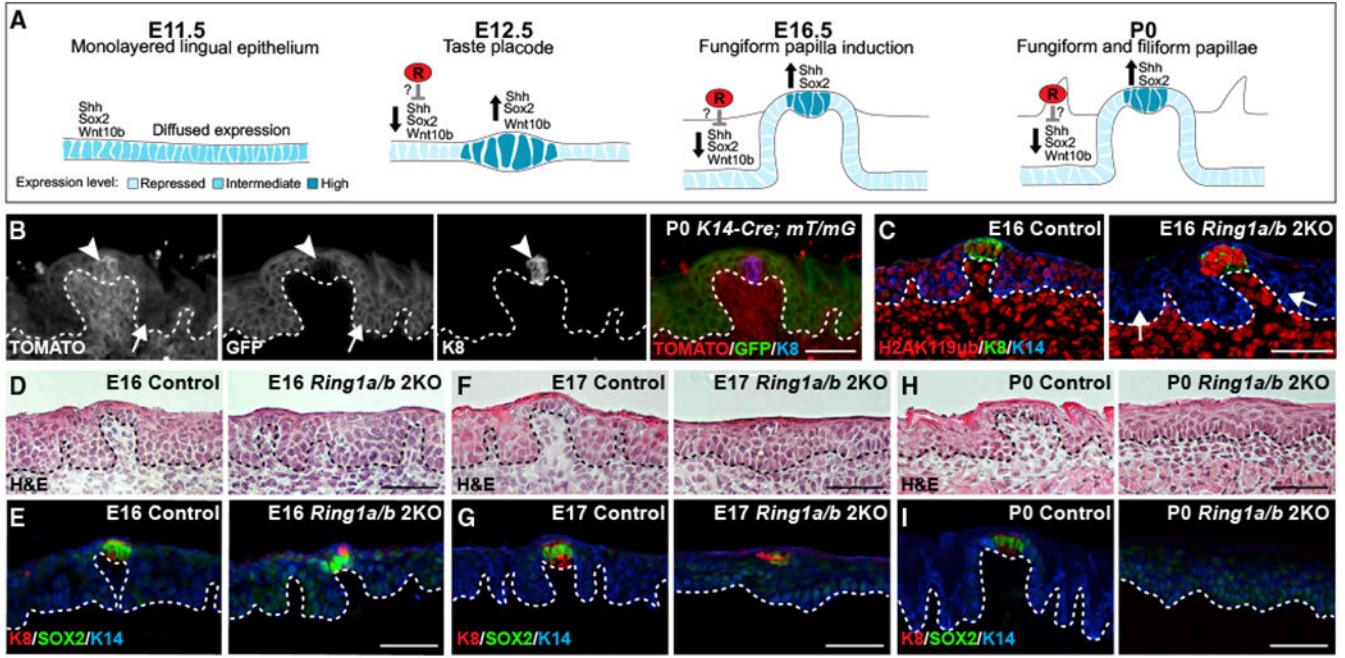
Highlights

- PRC1 is critical for lingual papillae development, while PRC2 is dispensable

- PRC1 ablation results in ectopic SHH signaling and taste cell niche collapse

- Ablation of SHH signaling in PRC1-null tongues rescues taste cell cluster integrity

- Spatial gene regulation in the non-gustatory niche is essential for taste cells

Figure 1. Ablation of *Ring1a/b* in the Non-gustatory Lingual Epithelium Results in a Progressive Loss of Fungiform Papillae and Ablation of Filiform Papillae

(A) Developmental timeline and gene expression pattern in the murine lingual epithelium (see text for details). R, repressor.

(B) Expression of the basal epithelial *K14-Cre* driver in control neonatal (P0) lingual epithelium, visualized by the *Rosa26-mT/mG* reporter.

(C) Immunofluorescence (IF) analysis of the H2AK119ub mark in the lingual epithelium of control and *Ring1a/b* 2KO E16 embryos.

(D–I) H&E analysis of control and *Ring1a/b* 2KO lingual epithelium (D, F, and H). (E, G, and I) IF analysis of taste cell markers SOX2 and K8 in control and *Ring1a/b* 2KO lingual epithelium at E16 (D and E), E17 (F and G), and P0 (H and I).

Arrowheads indicate taste cell clusters. Arrows indicate the non-gustatory epithelium. Dashed lines label the basement membrane. All IF and bright-field scale bars are 50 μm.
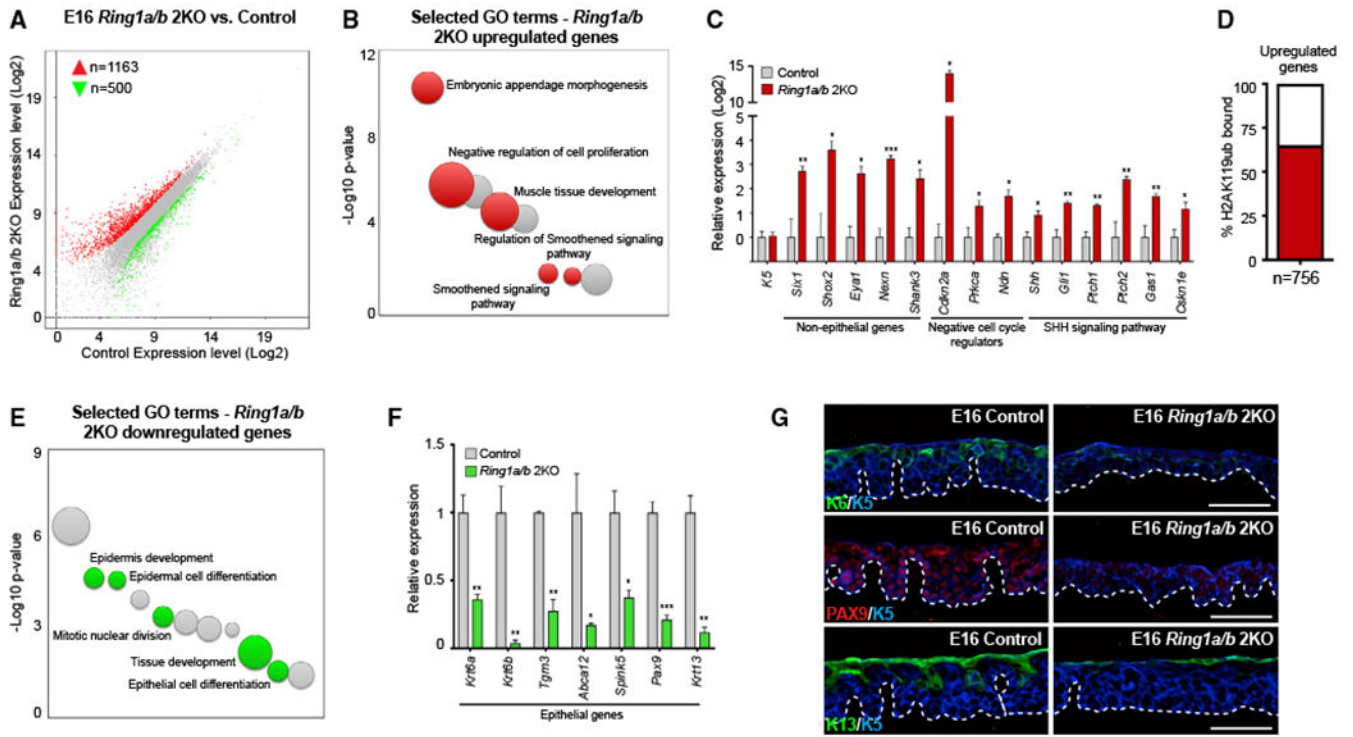
Figure 2. Cell-Cycle Repressors and SHH Signaling Components Are Upregulated in PRC1 Null Non-gustatory Epithelium

(A) Differential expression analysis in E16 *Ring1a/b* 2KO versus control in FACS-purified lingual epithelial cells. Genes with absolute fold change 1.8 and a false discovery rate (FDR) < 0.05 were considered upregulated (red) or downregulated (green). n = 2 embryos per genotype.

(B) Gene Ontology (GO) analysis of E16 *Ring1a/b* 2KO upregulated genes. Selected terms are labeled in red.

(C) qPCR analysis of selected genes in GO-enriched categories in *Ring1a/b* 2KO upregulated genes.

(D) Percentage of H2AK119ub-bound genes among *Ring1a/b* 2KO upregulated genes.

(E) GO analysis of E16 *Ring1a/b* 2KO downregulated genes. Selected terms are labeled in green.

(F) qPCR analysis of selected genes in GO-enriched categories in *Ring1a/b* 2KO downregulated genes.

(G) IF analysis of downregulated lingual keratinocyte markers K6, PAX9, and K13 in E16 control and *Ring1a/b* 2KO embryos. Dashed lines label the basement membrane. IF scale bars are 50 μm.

Data in graphs (C) and (F) are mean ± SEM. Data were analyzed by two-tailed Student's t test, *p < 0.05, **p < 0.01, ***p < 0.001. n = 3 embryos per genotype.
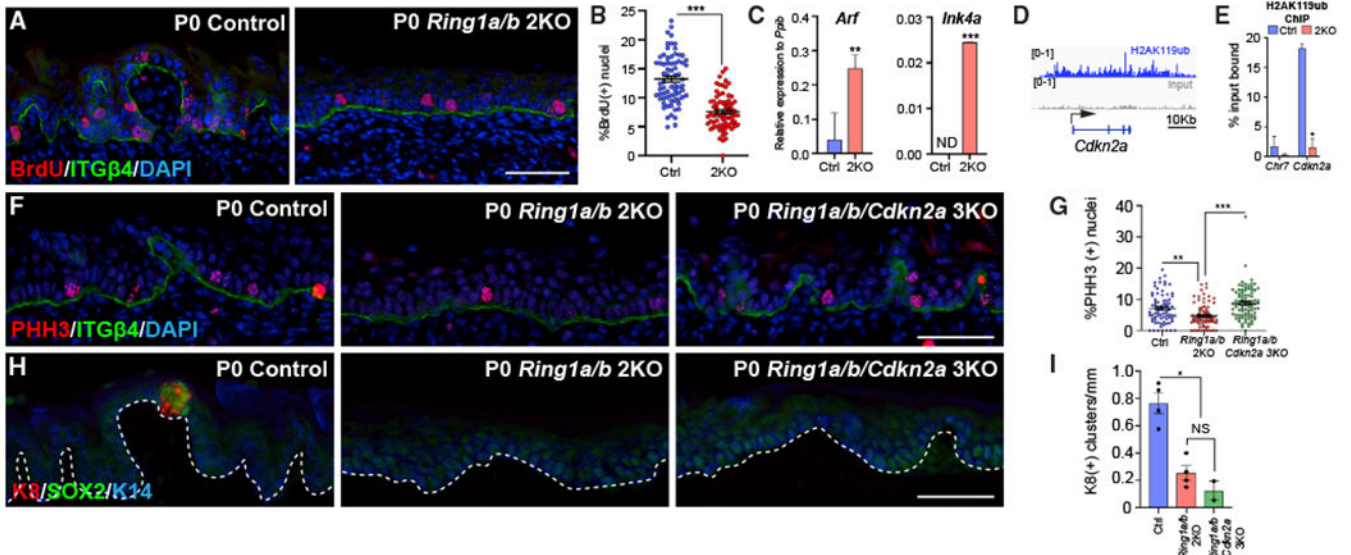
Figure 3. Loss of Lingual Papillae in *Ring1a/b* 2KO Mice Is Not Caused by *Cdkn2a* Upregulation Alone

(A) BrdU incorporation assay in P0 control and *Ring1a/b* 2KO tongues. Integrin β4 (ITGβ4) marks the basement membrane.

(B) Quantification of BrdU incorporation. Two-tailed Student's t test, ***p < 0.0001. n = 3 animals per genotype. Data are mean ± SEM.

(C) Expression levels of *Arf* and *Ink4a* relative to the housekeeping gene *Ppib* in E16 control and *Ring1a/b* 2KO FACS-purified lingual epithelium. Two-tailed Student's t test, **p < 0.001, ***p < 0.0001. ND, signal not detected, n = 4 embryos per genotype. Data are mean ± SD.

(D) Integrative Genomics Viewer (IGV) browser view of H2AK119ub and input for the *Cdkn2a* locus. Arrow indicates the transcription start site (TSS).

(E) P0 H2AK119ub ChIP-qPCR analysis on FACS-purified lingual epithelium of control and *Ring1a/b* 2KO mice for *Cdkn2a*. Two-tailed Student's t test, *p < 0.05. n = 2 ChIP replicates. Data are mean ± SEM.

(F) IF analysis of mitotic marker phospho-histone H3 (PHH3) in P0 control, *Ring1a/b* 2KO, and *Ring1a/b/Cdkn2a* 3KO tongues.

(G) Quantification of PHH3-positive cells. One-way ANOVA, **p < 0.005, ***p < 0.0005. n = 2 animals per genotype. Data are mean ± SEM. See STAR Methods for quantification details.

(H) IF analysis of taste cell markers SOX2 and K8 in P0 control, *Ring1a/b* 2KO, and *Ring1a/b/Cdkn2a* 3KO tongues.
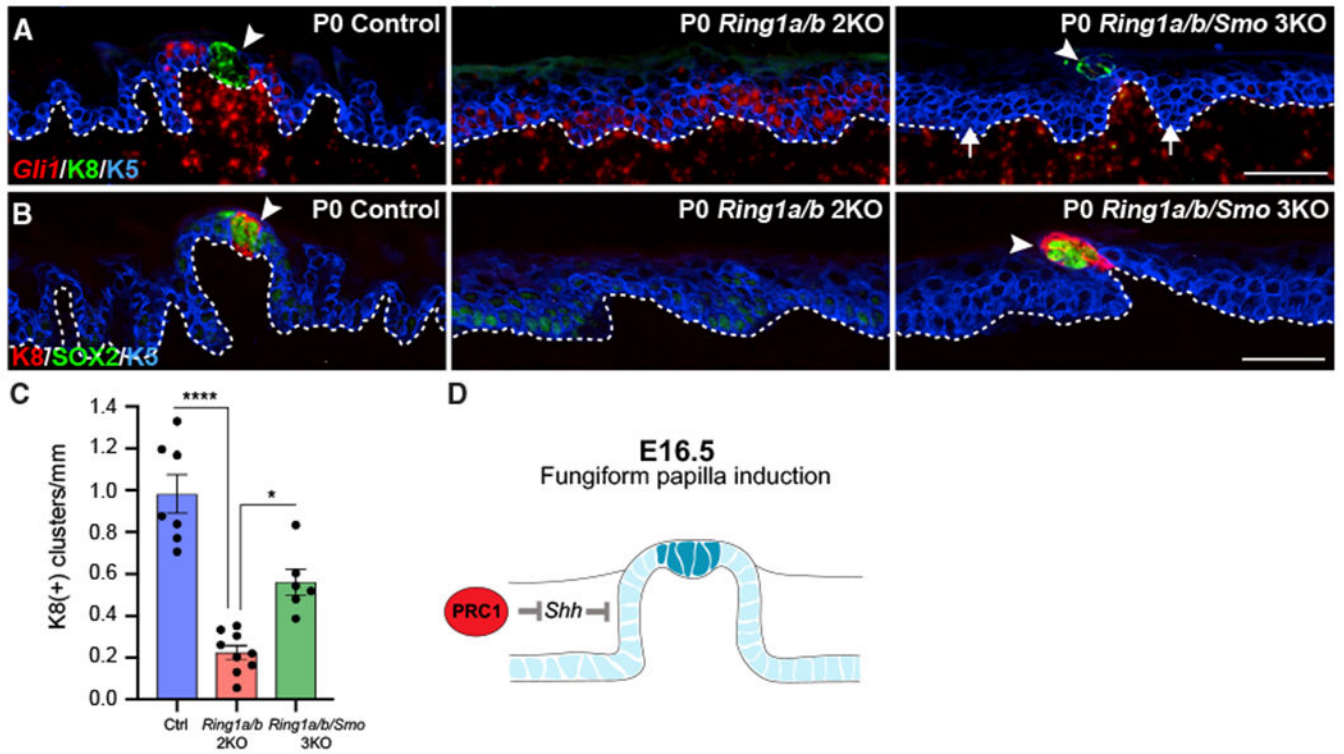
(I) Counts of K8(+) cell clusters per millimeter in P0 control, *Ring1a/b* 2KO, and *Ring1a/b/Cdkn2a* 3KO tongues. The bar represents the average of all animals, and data points are the quantification average of individual animals (n). One-way ANOVA (Kruskal-Wallis), *p < 0.05. NS, non-significant. Data are mean ± SEM.

See STAR Methods for quantification details. Dashed lines label the basement membrane. IF scale bars are 50 μm.
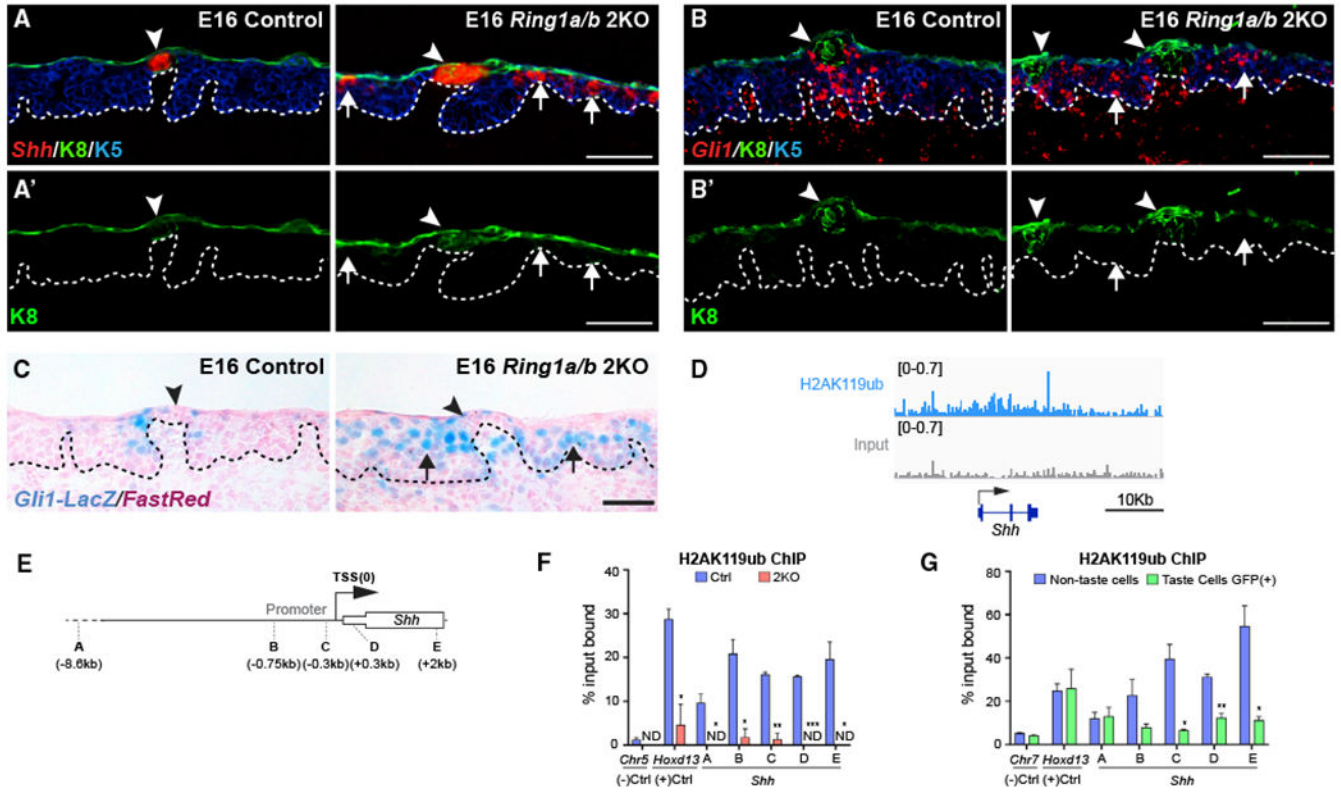
Figure 4. PRC1 Restricts SHH Signaling in the Non-gustatory Epithelium

(A and A′) *In situ* hybridization of *Shh* in E16 control and *Ring1a/b* 2KO tongues, co-stained with taste cell marker K8 and basal epithelial marker K5 (A). K8 channel alone (A′).

(B and B′) *In situ* hybridization of *Gli1* in E16 control and *Ring1a/b* 2KO tongues, co-stained with taste cell marker K8 and basal epithelial marker K5 (B). K8 channel alone (B′).

(C) Analysis of the SHH signaling reporter *Gli1-LacZ* in E16 control and *Ring1a/b* 2KO tongues. Nuclei are counterstained with fast red dye.

(D) IGV browser view of H2AK119ub and input for the *Shh* locus. The arrow indicates the transcription start site (TSS).

(E) Map of ChIP-qPCR primer locations on the *Shh* locus and surrounding areas.

(F and G) H2AK119ub ChIP-qPCR analysis of *Shh* in P0 control and *Ring1a/b* 2KO FACS-purified lingual epithelium. n = 2 ChIP replicates (F). H2AK119ub ChIP-qPCR analysis of *Shh* in FACS-purified TCF/LEF:H2B-GFP(+) taste cells and TCF/LEF:H2B-GFP(—) lingual keratinocytes. n = 2 ChIP replicates (G). Two-tailed Student's t test, *p < 0.05, **p < 0.01, ***p < 0.001. ND, signal not detected.

Image arrowheads indicate taste cell clusters, and arrows indicate the non-gustatory epithelium. Data in (F) and (G) are mean ± SEM. Dashed lines label the basement membrane. Bright-field and IF scale bars are 50 μm.

Figure 5. PRC1-Mediated Repression of SHH Signaling in the Non-gustatory Epithelium Is Critical for Fungiform Papillae Maintenance

(A) *In situ* hybridization analysis of *Gli1* in P0 control, *Ring1a/b* 2KO, and *Ring1a/b/Smo* 3KO tongues, co-stained with taste cell marker K8 and basal epithelial marker K5.

(B) IF analysis of taste cell markers SOX2 and K8 in P0 control, *Ring1a/b* 2KO, and *Ring1a/b/Smo* 3KO tongues.

(C) Counts of K8(+) cell clusters per millimeter in P0 control, *Ring1a/b* 2KO, and *Ring1a/b/Smo* 3KO tongues. The bar represents the average of all animals, and data points are the quantification average of individual animals (n). One-way ANOVA (Kruskal-Wallis), *p < 0.05, ****p < 0.0001. Data are mean ± SEM. See STAR Methods for quantification details.

(D) Model for PRC1 regulation in the non-gustatory epithelium (see text for details). Dashed lines label the basement membrane. Arrowheads indicate taste cell clusters. Arrows indicate the non-gustatory epithelium. IF scale bars are 50 μm.

KEY RESOURCES TABLE

REAGENT or RESOURCE	SOURCE	IDENTIFIER
Antibodies		
Rabbit anti-H2AK119ub	Cell Signaling	Cat# 8240S; RRID: AB_10891618
Rabbit anti-H3K27me3	Millipore	Cat# 07-449; RRID: AB_310624
Rabbit anti-Ring1b	Cell Signaling	Cat# 5694S; RRID: AB_10705604
Rabbit anti-Keratin 5	Elaine Fuchs lab	N/A
Chicken anti-Keratin 5	BioLegend	Cat# 905901; RRID: AB_2565054
Rabbit anti-Keratin 6	Elaine Fuchs lab	N/A
Rabbit anti Phospho histone H3	Upstate	Cat# 06-570; RRID: AB_310177
Rabbit anti RFP	MBL	Cat# PM005; RRID: AB_591279
Chicken anti GFP	Abcam	Cat# ab13970; RRID: AB_300798
Guinea pig anti-Keratin 13	Acris	Cat #BP5076; RRID: AB_979608
Chicken anti-Keratin 14	Julie Segre lab	N/A
Rat anti-Itgb4 (CD104)	BD Biosciences	Cat# 553745; RRID: AB_395027
Sheep anti-BrdU	Abcam	Cat# ab1893; RRID: AB_302659
Rat anti-Pax9	Abcam	Cat #ab28538; RRID: AB_777111
Rabbit anti-Sox2	Stemgent	Cat# 09-0024; RRID: AB_2195775
Rat anti-Keratin 8	DSHB	TROMA-1
Anti-Chicken Alexa Fluor 594	Jackson ImmunoResearch	Cat# 703-585-155; RRID: AB_2340377
Anti-Rabbit Alexa Fluor 594	Jackson ImmunoResearch	Cat# 711-585-152; RRID: AB_2340621
Anti-Rabbit Alexa Fluor 647	Jackson ImmunoResearch	Cat# 711-605-152; RRID: AB_2492288
Anti-Rat Alexa Fluor 647	Jackson ImmunoResearch	Cat# 712-605-150; RRID: AB_2340693
Anti-Chicken Alexa Fluor 488	Jackson ImmunoResearch	Cat# 703-545-155; RRID: AB_2340375
Anti-Rat Alexa Fluor 488	Jackson ImmunoResearch	Cat #711-545-152; RRID: AB_2313584
Anti-Guinea pig Alexa Flour 488	Jackson ImmunoResearch	Cat # 706-545-148; RRID: AB_2340472
APC anti-mouse CD326 (Epcam)	BioLegend	Cat# 118214; RRID: AB_1134102
Chemicals, Peptides, and Recombinant Proteins		
Dispase II	Thermo Fisher	Cat# 17105041
Collagenase, type 1	Worthington	Cat# L004196
Pierce 16% Formaldehyde (w/v), Methanol-free	Thermo Fisher	Cat# 28906
Glutaraldehyde 50%, EM grade	Electron Microscopy Sciences	Cat# 16320
Critical Commercial Assays		
Zombie Violet Fixable Viability Kit	BioLegend	Cat# 423113
In Situ Cell Death Detection Kit, Fluorescein	Roche	Cat# 11684795910
RNeasy Plus Micro Kit	QIAGEN	74034
qScript cDNA SuperMix	Quanta	95048
LightCycler® 480 SYBR Green I Master mix	Roche	04707516001
Ovation RNA-seq System V2	Nugen	7102

REAGENT or RESOURCE	SOURCE	IDENTIFIER
Ovation Ultra Low DR Multiplex system	Nugen	0329-96
Agencourt AMPure XP	Beckman Coulter	A63880
Dynabeads protein G	Invitrogen	10004D
ChIP DNA Clean and Concentrator kit	Zymo Research	D5205
DNA SMART ChIP-Seq Kit	Clontech	634872
RNAscope® 2.5 HD Reagent Kit - RED	RNAscope	322350
RNAscope Probe - Mm-Shh	RNAscope	314361
RNAscope Probe - Mm-Gli1	RNAscope	311001
RNAscope® Protease III & IV Reagents	RNAscope	322340
Deposited Data		
ChIP-seq data	This paper	GEO: GSE123095
RNA-seq data	This paper	GEO: GSE123095
Experimental Models: Organisms/Strains		
Mouse: Tg(*Krt14-Cre*)1Amc/J	Jackson Labs	004782
Mouse: *Tg(TCF/Lef1-HIST1H2BB/EGFP)61Hadj/J*	Jackson Labs	013752
Mouse: *Gli1^{tm2Alj}/J*	Jackson Labs	008211
Mouse: *Smo^{tm2Amc}/J*	Jackson Lab	004526
Mouse: *Gt(ROSA)26Sor^{tm4(ACTB-tdTomato,−EGFP)Luo}/J*	Jackson Lab	007576
Mouse: *Ring1a^{−/−}*	del Mar Lorente et al., 2000	N/A
Mouse: *Ring1b^{flox/flox}*	Cales et al., 2008	N/A
Mouse: *Ink4a/Arf^{−/−}*	Serrano et al., 1996	N/A
Mouse: *Eed^{flox/flox}*	Mu et al., 2014	N/A
Oligonucleotides		
Primers for mouse genotyping, see Table S4	This Paper	N/A
Primers for RT-qPCR, see Table S4	This paper	N/A
Primers for ChIP-qPCR, see Table S4	This Paper	N/A
Software and Algorithms		
DAVID v6.8	Huang da et al., 2009	https://david.ncifcrf.gov/
Bowtie v1.1.1	John Hopkins University	http://bowtie-bio.sourceforge.net/index.shtml
Bowtie v2.2.3	John Hopkins University	http://bowtie-bio.sourceforge.net/bowtie2/index.shtml
Samtools v0.1.19	Li et al., 2009	http://www.htslib.org/
Integrative Genomics Viewer (IGV)	Broad Institute	http://software.broadinstitute.org/software/igv/
igvtools v2.3.57	Broad Institute	https://software.broadinstitute.org/software/igv/igvtools
Tophat v2.0.13	John Hopkins University	https://ccb.jhu.edu/software/tophat/index.shtml
cufflinks v2.2.1	Trapnell Lab	http://cole-trapnell-lab.github.io/cufflinks/
HTSeq v0.6.1	Anders et al., 2015	https://github.com/simon-anders/htseq
DESeq2 v1.6.3	Love et al., 2014	http://www.bioconductor.org/packages/release/bioc/html/DESeq2.html